

# Hierarchical-Variational Mode Decomposition for Baseline Correction in Electroencephalogram Signals

SHIREEN FATHIMA<sup>1,2</sup> AND MAAZ AHMED<sup>2</sup>

<sup>1</sup>Faculty of Electrical and Electronics Engineering Sciences, Visvesvaraya Technological University, Belagavi 590018, India

<sup>2</sup>Department of Electronics and Communication Engineering, HKBK College of Engineering, Bengaluru 560045, India

CORRESPONDING AUTHOR: S. FATHIMA (e-mail: shireen.fathima6@gmail.com)

**ABSTRACT** Electroencephalogram (EEG) signals being time-resolving signals, suffer very often from baseline drift caused by eye movements, breathing, variations in differential electrode impedances, movement of the subject, and so on. This leads to misinterpretation of the EEG data under test. Hence, the absence of techniques for effectively removing the baseline drift from the signal can degrade the overall performance of the EEG-based systems. To address this issue, this article deals with developing a novel scheme of hierarchically decomposing a signal using variational mode decomposition (VMD) in a tree-based model for a given level of the tree for accurate and effective analysis of the EEG signal and research in brain-computer interface (BCI). The proposed hierarchical extension to the conventional VMD, i.e., H-VMD, is evaluated for performing baseline drift removal from the EEG signals. The method is tested using both synthetically generated and real EEG datasets. With the availability of ground-truth information in synthetically generated data, metrics like percentage root-mean-squared difference (PRD) and correlation coefficient are used as evaluation metrics. It is seen that the proposed method performs better in estimating the underlying baseline signal and closely resembles the ground truth with higher values of correlation and the lowest value of PRD when compared to the closely related state-of-the-art methods.

**INDEX TERMS** Baseline drift, electroencephalogram (EEG), intrinsic mode functions (IMFs), variational mode decomposition (VMD).

## I. INTRODUCTION

ELECTROENCEPHALOGRAM (EEG) is a method of measuring the electric potentials generated in the brain for the analysis of normal and abnormal brain activities. The advancements and convenience in noninvasive EEG systems have made their applications possible beyond medical applications in domains like gaming [1], motor imagery [2], learning [3], security applications [4], brain-computer interfaces (BCIs), and so on. However, the real-time application of EEG is very challenging due to the noise or artifacts [5] which are undesired components arising because of muscle movements, line noise, breathing, heart rate, eye blinks, and so on; they mislead the actual cerebral activity of the recorded EEG data leading to

complexity in analyzing the EEG data and often result in drifting the baseline of the EEG [6], [7]. Baseline drifts in EEG are slow varying waves and are transient patterns that are sharply countered. Poor contact of electrodes, varying pressure of electrode contact, electrode impedance, changes in skin resistance, variations in temperature, bias in amplifiers, and instrumentation also culminates in drifting of the baseline [8], [9]. Baseline drifts are common in many physiological signals like electrocardiography (ECG) [10] and electrooculography (EOG) [9]. In ECG, baseline drift leads to incorrect diagnosis of cardiovascular diseases [10] under consideration; while in EOG, the baseline drift may yield incorrect estimation of the subject's point of gaze [9]. Baseline drift in EEG leads to severe confusion

in interpreting the data in experiments like power spectral analysis [11] or event-related potential (ERP) analysis [12] while also causing alterations in computing the signals. Storing large amounts of EEG data in such cases creates the overhead of memory management as encoding higher amplitudes of EEG requires more bits [11]. Hence, the preprocessing stage of EEG should include the correction of baseline drifts [8] immediately after extracting epochs from the continuous EEG data to simplify further processing of the signal, quantifying the parameters, and extracting features. Two inherent challenges in baseline correction are the choice of baseline interval and the assumption that there are no systematic differences between conditions in the baseline interval. Baseline correction usually consists of using EEG activity before an external event occurs, i.e., over a baseline period to correct activity over a post-stimulus interval, i.e., the time after an external event occurs. The motivation behind the removal of baseline drift is to process the EEG signals before feature extraction. The subject-specific noise in the EEG signal will be removed by baseline correction thus resulting in subject-independent features making the analysis and computations easier. Baseline correction transforms all power data to the same scale allowing us to compare, visually and statistically, results from different frequency bands, electrodes, conditions, and subjects. It also makes parametric statistical analyses appropriate to use as baseline corrected data are often normally distributed.

In this article, we propose a variant of the variational mode decomposition (VMD) method for baseline drift correction in the EEG signals. Here, the signal is hierarchically decomposed into several mode functions and the baseline signal is reconstructed based on the mean frequency of the intrinsic mode functions (IMFs) in the hierarchy decided by the first IMF. For evaluation of the accuracy of the proposed method from a computational analysis viewpoint, simulations on synthetic EEG data and the Covert Shift Dataset are carried out. The proposed method is compared with existing approaches using the performance parameters, such as percentage root-mean-squared difference (PRD) and correlation coefficient.

The remainder of this article is organized as follows. Section II gives a brief description of the related work on baseline correction. Section III describes the methodology of the proposed work. Section IV discusses the performance results of the proposed method and comparative performance analysis with the existing works evaluated on different EEG signals taken from publicly available databases and self-acquired data. Section V concludes this article along with the future roadmap of the study.

## II. RELATED WORK

Many existing methods for correcting the baseline drift from physiological signals rely mostly on low-pass filtering. Such methods extract the baseline drift via low-pass filtering and subtract it from the given signal under test. Filters designed with constant cut-off frequency are incapable of removing

the baseline drift [11]. The properties of the filter must be adaptive to the local spectral contents of the baseline drift. Some of the very earlier works based on low-pass filtering are as follows. The works of Zhou et al. [13] are based on the segmentation of cubic and parabola functions in correcting ECG baseline drift using an adaptive dual threshold method. The works of Tkacz [14] made use of single-moving average filtering to compute the baseline drift. Finite impulse response filters formed by cascading several moving average filters, and a short corrector filter using an algorithm that determined the best linear-phase corrector filter for any given cutoff frequency, sampling frequency, set of tap weights, and lengths of the moving average filters were employed in the works of Riccio and Belina [15] to ECG signals for correcting baseline drift. The limitation of this filter design method was the time required to determine an optimal system given the required parameters of sampling frequency, cutoff frequency, and so on. Moreover, such methods work best for signals having less frequency variations. But it does not necessarily hold true to EEG signals as they have many time-varying spectral components inherent in them. This increases the complexity of estimating the baseline drift in EEG. Another class of earlier attempts dealt with adaptive mechanisms that mainly depended on a presumed reference signal [16], [17], however, the need of reference signals makes these approaches inaccessible in many cases. Another notable earlier method in EEG baseline correction is in the adaptive filter designs by polynomial warping by Philips [7] where a time-warped polynomial filter (TWPF) was proposed as a new interval adaptive filter that reacts immediately to changes in the signal's properties, independently of the desired noise reduction and does not require a reference signal. However, this technique limited its applicability as it required the power of nonstationary components to be larger than stationary components, and also the technique could only separate out the stationary from nonstationary components. Owing to the nonstationary nature, the problem of baseline drift removal is not a straightforward approach in the domain of EEG. However, there have been tremendous works in baseline drift removal research in ECG signals owing to their repetitive nature. Also most of these ECG-based algorithms are variants of empirical mode decomposition (EMD), such as fractality and EMD combined to remove baseline drift as in [18] where the drift is modeled as fractional Brownian motion process, multivariate EMD [19] where only two higher indexed IMFs corresponding to the lowest frequency contents were used, wavelet and EMD [20] where EMD is employed as an adaptive technique for signal decomposition, and DWT is used for denoising based on a given thresholding criterion, selection of certain components of EMD [21] that dealt with nonlinear and nonstationary signals, summing up of EMD components up to a certain minimum range of frequencies [22], and so on. As these methods largely depend on EMD, they tend to suffer in the presence of noise [23] and lack mathematical theoretical support. Also,

since EMD is recursive in nature, it does not permit the correction of backward error. Hence, in one of the recent works, Prabhakararao and Manikandan [10] used VMD and selected the first component of VMD as the baseline drift. However, in our study related to EEG, we found that the first component of VMD cannot represent the baseline drift completely (as in [10] for ECG) as the muscle artifacts like blinks become dominant in the bandwidth of the first component. Hence, the current study aims at effectively removing the baseline drift in EEG signals with a novel extension to the conventional VMD algorithm to decompose the signal hierarchically into IMFs.

### III. METHODOLOGY

This section briefs the proposed method of hierarchically decomposing a signal into its constituent IMFs using VMD. VMD is a nonrecursive technique which can derive the underlying structure of a nonstationary signal by signal decomposition. The VMD algorithm decomposes a 1-D time series into  $K$  number of modes  $u_k(t)$  as,  $x(t) = \sum_{k=1}^K u_k(t)$ , with the criterion that the signal gets reconstructed ideally fully by summing up the  $K$  number of modes while the sum of bandwidths of all modes is kept minimum [24]. The decomposed signal is a series of IMF in different frequency bands, each IMF has its own exclusive limited bandwidth, and the central frequency of each bandwidth is different. Every mode is compact along the mean frequency  $\omega_k$  and can be represented by frequency and amplitude modulation properties. The method solves a constrained variational function to find optimal  $\omega_k$  and  $u_k$  given by

$$\min \left\{ \left\| \sum_k \partial_t \left[ \left( \partial(t) + \frac{j}{\pi t} \right) * u_k(t) e^{-j\omega_k t} \right] \right\|_2^2 \right\}$$

subject to the condition  $\sum_k u_k = x$  (1)

where  $\{u_k\} = \{u_1, u_2, \dots, u_k\}$  are the decomposed mutually independent frequency band components, and  $\{\omega_k\} = \{\omega_1, \omega_2, \dots, \omega_k\}$  are corresponding central frequency.  $\delta(t)$  is unit impulse function,  $\delta_t$  is the gradient with respect to time, and  $x$  is the input signal to be decomposed. The symbol  $*$  refers to the convolution operation.

The solution to the constrained optimization problem mentioned above is obtained by the use of Lagrange multipliers which enforces the reconstruction constraint and quadratic penalty which increases the convergence of the solution. This results in an unconstrained problem defined as

$$L(\{u_k\}, \{\omega_k\}, \lambda) = \alpha \sum_{k=1}^K \left\| \partial_t \left[ \left( \partial(t) + \frac{j}{\pi t} \right) * u_k(t) e^{-j\omega_k t} \right] \right\|_2^2 + \left\| f(t) - \sum_{k=1}^K u_k(t) \right\|_2^2 + \lambda (f(t) - \sum_{k=1}^K u_k(t))$$
 (2)

The optimal center frequency is obtained by minimizing the above Lagrangian that means to find the saddle point by

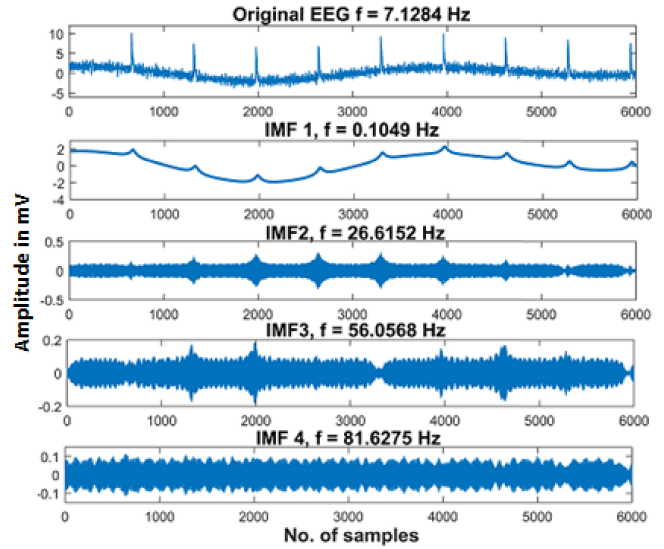


FIGURE 1. Decomposition of a raw EEG signal into its constituent IMFs using VMD.

using the alternate direct method of multipliers (ADMMs) in a series of iterations that can be summarized as follows.

- 1) *Modes Updating*: An embedded Weiner filter is used to update the modes in the frequency domain centered at the corresponding center frequencies as

$$\hat{u}_k^n + 1 = \frac{\hat{f} - \sum_{i < k} \hat{u}_i^{n+1} - \sum_{i < k} \hat{u}_i^n + \frac{\lambda^n}{2}}{1 + 2\alpha(\omega - \omega_k^n)^2}.$$
 (3)

- 2) *Center Frequency Updating*: The center of gravity of a mode's power spectrum is updated as center frequency given as

$$\omega_k^{n+1} = \frac{\int_0^\infty \omega |\hat{u}_k^{n+1}(\omega)|^2 d\omega}{\int_0^\infty |\hat{u}_k^{n+1}(\omega)|^2 d\omega}.$$
 (4)

- 3) *Lagrangian Multiplier Update*: The Lagrangian multiplier is updated until  $\sum_k \|\hat{u}_k^{n+1} - \hat{u}_k^n\|_2^2 \leq \epsilon$  as

$$\hat{\lambda}^{n+1} = \hat{\lambda}^n + \tau \left( \hat{f} - \sum_k \hat{u}_k^{n+1} \right)$$
 (5)

where  $n$  denotes the iteration number,  $\alpha$  is the data fidelity parameter, and  $\lambda$  is the Lagrangian multiplier. The reader is requested to get the detailed explanation of the VMD algorithm from [24]. Fig. 1 shows the decomposition of a raw EEG signal into its four constituent IMFs as a function of its mean frequency. The mean frequency of the signal is calculated as

$$f(\omega) = \frac{\sum_{i=0}^{n-1} I_{\omega(i)} f_{\omega(i)}}{\sum_{i=0}^{n-1} I_{\omega(i)}}$$
 (6)

where  $n$  is the number of frequency bins,  $\omega_i$  is the frequency band at bin  $i$ ,  $f_{\omega(i)}$  is the frequency, and  $I_{\omega(i)}$  is the energy density of  $\omega$  at frequency bin  $i$ . The values of the mean frequencies are given on each subplot in Fig. 1.

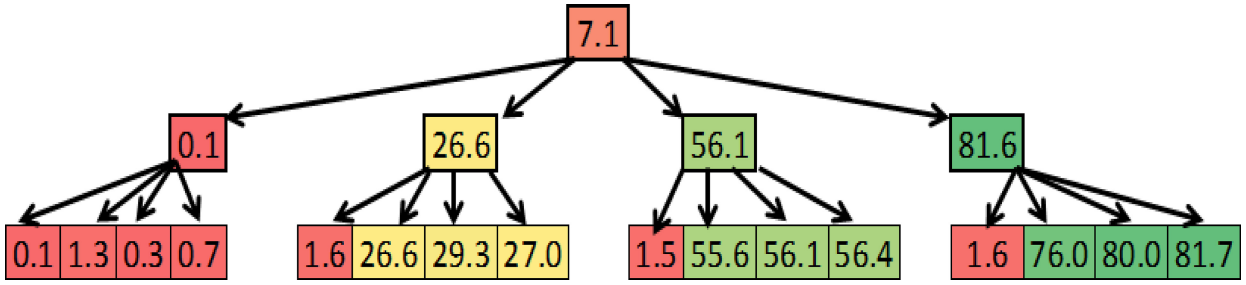


FIGURE 2. Heatmap of mean frequencies across different nodes in H-VMD for a sample EEG data. Color coding: red to green for lower to higher values, respectively.

The EEG signal is decomposed into four IMFs in VMD based on extensive empirical studies so that the lower frequency components, such as theta and delta rhythms of EEG, are captured by the first mode and the higher frequency components, such as beta and gamma rhythms, are captured by the fourth IMFs resulting in maximum frequency separation between the modes and making four IMFs sufficient to segregate the baseline wander. A large number of  $K$  yields IMFs which are mostly identical and a smaller number of  $K$  will result in poor segregation of IMFs.

Fig. 2 shows the tree hierarchy of the decomposed IMFs through a heatmap scheme of the mean frequencies obtained at different nodes and levels of the tree model. It is to be noted as to how the values of mean frequency are lesser for the left children nodes of a given parent node in comparison to their rightmost children in the tree architecture.

#### A. PROPOSED HIERARCHICAL-VMD

This section briefs the concerns of applying VMD to remove baseline drift in EEG signals and presents a pseudocode of the proposed hierarchical-VMD (H-VMD) algorithm. The overall implementation of H-VMD is defined in the pseudocode given below. Lines 1–12 in the algorithm represent the decomposition of a signal at various levels and the construction of tree hierarchy. Line 6 uses the VMD function implementation as given in [24]. The reconstruction of the baseline using the constraint defined by (7) is done from lines 13 to 20.

It is seen in Fig. 1 that the IMFs obtained from VMD increase in their mean frequencies, i.e., higher frequency signals are obtained in higher IMFs. The first IMF captures the low-frequency components mostly delta and theta rhythms of EEG and looks somewhat like the baseline of the EEG, however, it contains the traces of blink or any other dominant muscle artifacts in it.

Based on this, the study in [10] used the first IMF as the baseline of the signal under test and subtracted it from the original signal to remove the baseline wander from the signal. However, it is to be observed that considering the first IMF as the baseline would remove other important parts of the signal. In Fig. 1, it can be seen that the first IMF has blink-type artifacts and hence, it cannot be used solely to determine the baseline drift of EEG. Hence, we formulate a

#### Algorithm 1 Baseline Wander Removal Using H-VMD

**Input:** Raw EEG data  $x[n]$  at sampling rate  $f_s$   
 $L \leftarrow$  level of the H-VMD tree  
 $\alpha \leftarrow$  Balancing parameter of data-fidelity constraint  
 $\tau \leftarrow$  time-step of dual ascent, 0 for noise-slack  
 $K \leftarrow$  number of modes  
 $DC \leftarrow$  true if the first mode is put and kept at DC (0-freq)  
 $Init \leftarrow$  all omegas start uniformly distributed  
 $tol \leftarrow$  tolerance of convergence criterion  
**Output:** EEG data,  $\hat{x}[n]$  without baseline wander artifact  
**Procedure:**  
1:  $u\{1\} \leftarrow x[n]$   
2:  $levels \leftarrow 1$   
3: **for**  $i = 2$  to  $L$  **do**  
4:    $indices = find(levels == (i-1))$   
5:   **for**  $idx = indices$  **do**  
6:      $s = VMD(u\{idx\}, \alpha, \tau, K, DC, init, tol)$   
7:     **for**  $k=1 : K$  **do**  
8:        $u = [u\{s(k:)\}]$   
9:     **end for**  
10:     $levels = [levels \ i * ones(1,K)]$   
11:   **end for**  
12: **end for**  
13. Reconstruction of baseline using mean frequency  $f$ ,  
14.  $baseline \leftarrow zeros(n,1)$   
15.  $\delta \leftarrow f(IMF_1)$   
16. **for**  $i=2 : \text{number of nodes}$  **do**  
17.   **if**  $f(u\{i\}) < \delta$  **then**  
18.      $baseline = baseline + u\{i\}$   
19.   **end if**  
20. **end for**

technique which uses the frequency information of the first IMF to decide which IMFs to consider to reconstruct the baseline from a hierarchy of available IMFs using VMD. Thus, the constraint used is given by

$$f(s) \leq f(IMF_1). \quad (7)$$

$\forall s$  being the hierarchical IMFs from the VMD tree.  $s \in U$ , the total available IMFs from the VMD tree as shown in Fig. 3. The original signal is placed at the root node-level 1 (shown in red in Fig. 3). The IMF whose mean frequency is lesser in level 2 is considered as the IMF1 shown in the



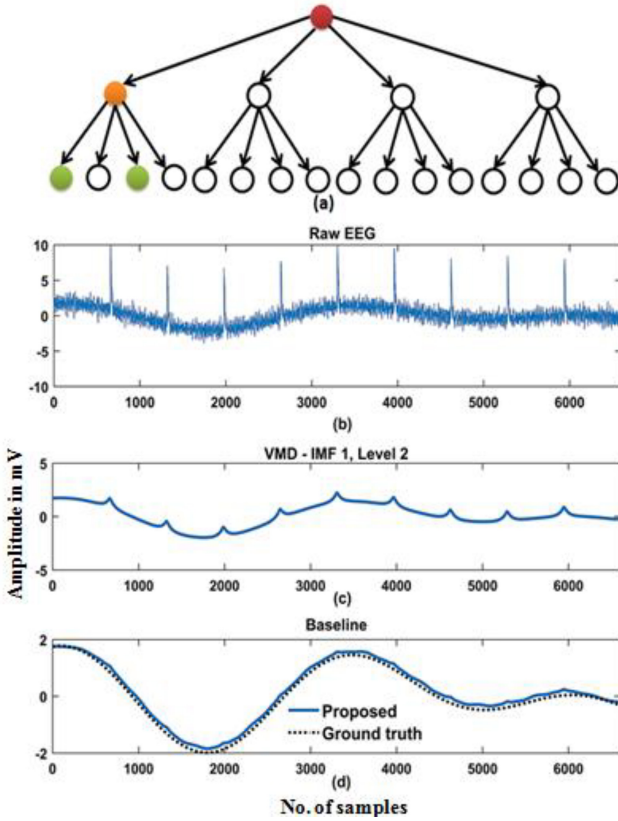


**FIGURE 3.** (a) VMD decomposition in a hierarchical manner with the red ball being the original raw signal shown in (b), orange ball—the 1st IMF shown in (c), and green balls—the IMFs satisfying the constraint given in (7). The baseline obtained by summing up these IMFs is shown in (d).

orange color in Fig. 3. Finally, the IMFs in  $U$  that satisfy the constraint given in (7) (shown in green) are summed up for the reconstruction of the baseline drift in the signal under test.

## B. DATASETS

We generated a synthetic EEG signal using the tools provided in [25]. Background EEG signal  $x(t)$  is generated such that its power spectrum matches the power spectrum of human EEG. Blink-type peaks were also added to simulate real-world scenarios as mentioned in [28]. As EEG baselines usually fall in the delta band (0–4 Hz), we generated the baseline in this range itself. This baseline is then added to the synthetic EEG. Mathematically, the baseline was modeled as

$$b(t) = \sum_{k=0}^K \sin(2 * \pi * f * t + \phi) \quad (8)$$

where  $b(t)$  is the baseline noise,  $f$  is the frequency in the delta band,  $K$  is the number of sinusoidal functions that can be placed within the chosen spectrum of baseline artifact, and  $\Phi$  is a random shift in phase in the interval  $[0, 2\pi]$  applied to each sine. An additive model created baseline

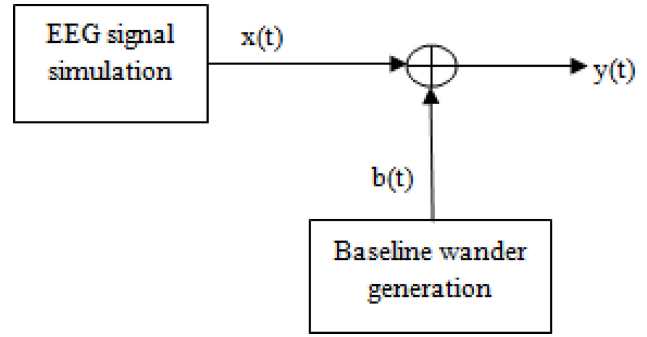


**FIGURE 4.** Additive model depicting the synthesis of EEG signal and baseline wander and their superposition to generate the baseline EEG.

EEG consisting of the sum of reference EEG signal  $x(t)$  and the baseline  $b(t)$  as

$$y(t) = x(t) + b(t). \quad (9)$$

Twenty such single-channel EEG data is created with a sampling frequency of 220 Hz and varying baseline in the delta band as depicted in Fig. 4. Thus, in this dataset, we have information of the ground-truth baseline. This effectively helps in the validation of related baseline removal algorithms.

Data from the Covert Shift Dataset [26] is used to show the baseline drift extraction capabilities of the proposed and the comparison algorithms. This dataset is an offline experiment wherein eight healthy participants, seven males and one female, aged 18–27 years, had to shift covert spatial attention to one out of six possible target directions while strictly fixating the center of the display. The EEG was recorded from Brain Products 64 channel actiCAP, digitized at a sample rate of 1000 Hz, with impedances kept below 20K. Each participant completed 600 trials in six blocks of 100 trials with 2-min breaks between blocks. This dataset is basically a high-end EEG dataset with data acquired at a sampling rate of 100 Hz.

## C. SIGNAL QUALITY EVALUATION METRICS

The metrics used in this study to assess the quality of the baseline extraction from the EEG signal is as follows. The PRD is used to quantitatively assess the difference between the original EEG  $x = x_1, x_2, \dots, x_N$  and the reconstructed EEG signal,  $\hat{x} = \hat{x}_1, \hat{x}_2, \dots, \hat{x}_N$ , given by

$$\text{PRD} = 100 \times \sqrt{\frac{\sum_{n=1}^N [x - \hat{x}]^2}{\sum_{n=1}^N [x]^2}}. \quad (10)$$

PRD provides a numerical measure of the residual root-mean-square error. Smaller values of PRD indicate lesser loss during the reconstruction phase. Next, we compute the correlation coefficient between  $x$  and  $\hat{x}$ . The correlation

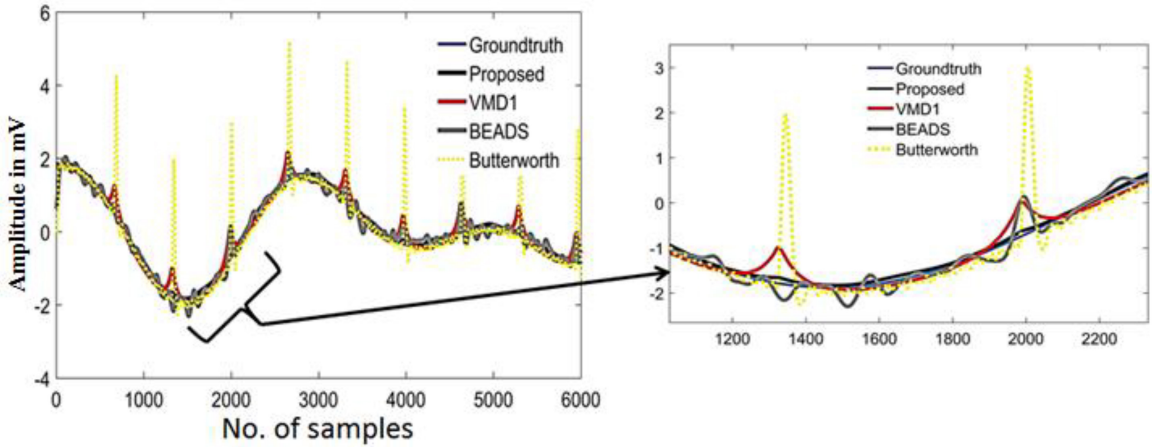


FIGURE 5. Baseline extraction from the proposed H-VMD and existing methods on the synthetic EEG data.

coefficient is the measure of similarity between the two signals under test and is given by

$$\rho = \frac{\sum (x_i - \bar{x})(\hat{x}_i - \bar{\hat{x}})}{\sqrt{\sum (x_i - \bar{x})^2(\hat{x}_i - \bar{\hat{x}})^2}}. \quad (11)$$

The higher the correlation between these two inputs, the better is the reconstruction. The percentage proportion of bandpower is computed in the five important EEG frequency bands, i.e., delta, theta, alpha, beta, and gamma bands. It is to be noted that as these metrics require the ground-truth baseline information, they can only be computed on the simulated EEG datasets. In case of real EEG, we show the visual comparison of reconstruction phases for the proposed and the existing methods.

#### IV. RESULTS AND DISCUSSION

The results are presented for H-VMD and are compared against the existing works. The notations used to denote each of these works are as follows. The algorithm in [10] which is based on using the first IMF of VMD is termed as VMD1. Here, the baseline wander is estimated by finding suitable tuning parameters for bandwidth constraint and number of modes and center frequency criterion of VMD. The works of Ning et al. [27] based on baseline estimation and denoising using sparsity is referred to as BEADS. This method is based on formulating a convex optimization problem designed to encapsulate nonparametric models of the baseline and the signal peaks. Specifically, the baseline is modeled as a low-pass signal and the series of signal peaks is modeled as sparse and as having sparse derivatives. The convex optimization problem and the properties of the majorization–minimization (MM) approach of the BEADS algorithm guarantee it to converge regardless of its initialization. The conventional Butterworth employed in [11] is termed as Butterworth which applies a standard low-pass Butterworth filter with normalized cutoff frequency in the range of 0.5–1.0 Hz and order being 3 to extract the baseline wander. It is

TABLE 1. Proportion of bandpower in five frequency bands by the percentage on the synthetic EEG data.

	delta [0-4Hz]	Theta [4-8Hz]	alpha [8-12Hz]	beta [12-20Hz]	Gamma [20-50Hz]
Original EEG	38.9 ±1.3	22.9 ±1.5	12.5 ±2.1	7.6 ±1.1	10.7 ±1.3
Baseline added	69.5 ±3.6	11.4 ±1.5	6.2 ±1.1	3.8 ±0.7	5.3 ±0.9
H-VMD	37.3 ±1.3	23.5 ±1.5	12.8 ±2.1	7.8 ±1.2	11.07 ±1.4
VMD1	28.7 ±1.1	26.2 ±1.7	14.6 ±2.4	8.9 ±1.3	12.7 ±1.6
BEADS	34.09 ±1.8	24.7 ±1.6	13.4 ±2.1	8.2 ±1.3	11.6 ±1.4
Butterworth	34.2 ±1.4	35.3 ±2.4	11.4 ±1.9	6.4 ±0.9	8.9 ±1.1

difficult to adapt the filter order dynamically and hence, a single optimum value based on the data is set for all the experimental runs.

##### A. ANALYSIS OF SYNTHETIC EEG DATA

Fig. 5 shows the performance of H-VMD and other related algorithms. The ground-truth baseline is given in black and it is to be noted that the baseline extracted by H-VMD closely resembles the ground truth in comparison to the rest of the methods. Fig. 6 shows a synthetic original EEG signal, the EEG signal added with ground-truth baseline is named Baseline EEG. It can be observed that the reconstructed EEG after extracting the baseline by using our proposed method resembles the original EEG signal.

The PRD analysis reveals that there is less difference between the ground-truth baseline and the one extracted using H-VMD (Fig. 7). The values of PRD are comparatively lesser for H-VMD than the other existing methods. On similar grounds, the correlation values of the extracted baselines using each of the methods against the ground-truth baseline are shown in Fig. 8. The correlation values obtained for H-VMD are higher than the other methods used. These

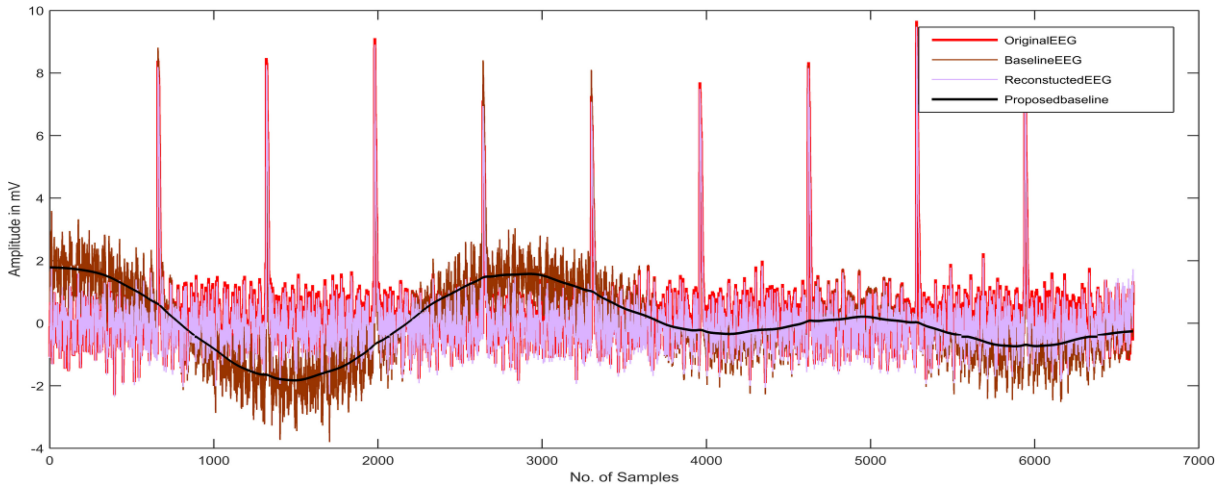


FIGURE 6. Extraction of baseline using the proposed method and the reconstructed signal.

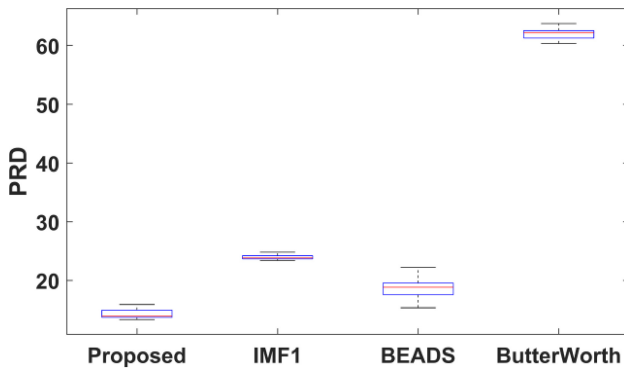


FIGURE 7. PRD values for the proposed H-VMD and the existing methods on the synthetic EEG data.

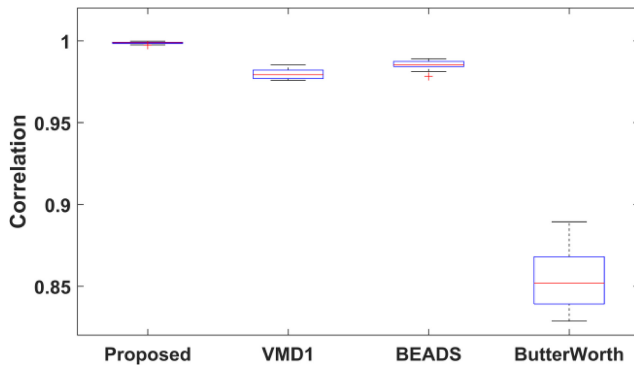


FIGURE 8. Correlation coefficient values for the proposed H-VMD and the existing methods on the synthetic EEG data.

two metrics show that the baseline extracted with H-VMD resembles the ground truth very well. Table 1 shows the frequency-domain analysis results for the extracted baselines. The percentage proportion of bandpower in the important EEG frequency bands is given for the original EEG, baseline added EEG, and then for the baseline extracted by different methods. The proportion values obtained using the H-VMD are very much similar to the values for the original EEG.

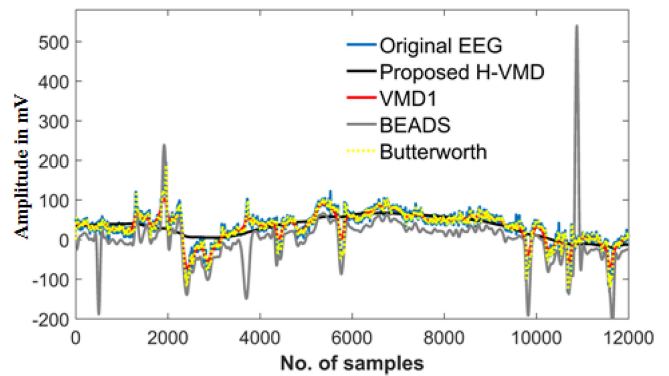


FIGURE 9. Baseline extraction from the proposed H-VMD and existing methods on the real EEG data.

Thus, the quantitative results provide a substantial agreement of the proposed method, as illustrated in Table 1.

## B. ANALYSIS OF REAL EEG DATA

Fig. 9 shows the baseline extraction obtained using the proposed method and the comparison algorithms on one sample EEG data taken from the Covert Shift Dataset. It is to be noted that the H-VMD is capable of extracting the baseline trend effectively in comparison to the rest of the methods even in the presence of sharp blink artifacts. The methods other than H-VMD seem to be easily biased with noise and hence, they resemble more like the raw EEG data in such cases. Similar trends are seen for the rest of the files and are omitted in this article for the sake of brevity.

## V. CONCLUSION AND FUTURE ROADMAP

Baseline drift is one of the common issues inherent in EEG signal analysis. In this article, we propose a novel scheme termed as H-VMD that hierarchically decomposes the EEG signal and estimates the baseline signal based on the mean frequency of the IMFs in the hierarchy. The extracted baseline can then be subtracted from the

original EEG signal to get a clean baseline-free EEG signal. The proposed method is compared systematically using synthetically generated EEG data with eye blink artifacts and baseline drifts. Comparison with other existing methods shows the robustness of the proposed scheme in estimating the baseline drift even in the presence of sharp blink artifacts. The method is also tested using the real EEG dataset and is found to be better than the existing methods. The algorithm in the present state consumes a considerable amount of computational resources and hence, as a future scope, we would like to develop a much faster version. Also, we would like to test the proposed method on other physiological signals like ECG and EOG.

## ACKNOWLEDGMENT

The authors thank their institute for providing the necessary amenities for carrying out this work.

## REFERENCES

- [1] G. U. Navalyal and R. D. Gavas, "A dynamic attention assessment and enhancement tool using computer graphics," *Human-Centric Comput. Inf. Sci.*, vol. 4, no. 11, pp. 1–7, 2014.
- [2] R. Bose, A. Khasnobish, S. Bhaduri, and D. N. Tibarewala, "Performance analysis of left and right lower limb movement classification from EEG," in *Proc. IEEE 3rd Int. Conf. Signal Process Integr. Netw. (SPIN)*, 2016, pp. 174–179.
- [3] A. Sinha, R. Gavas, D. Chatterjee, R. Das, and A. Sinharay, "Dynamic assessment of learners' mental state for an improved learning experience," in *Proc. IEEE Frontiers Educ. Conf. (FIE)*, 2015, pp. 1–9.
- [4] R. D. Gavas and G. U. Navalyal, "Fast and secure random number generation using low-cost eeg and pseudo random number generator," in *Proc. IEEE Int. Conf. Smart Technol. Smart Nation (SmartTechCon)*, 2017, pp. 369–374.
- [5] A. Sinha, D. Chatterjee, R. Das, S. Datta, R. Gavas, and S. K. Saha, "Artifact removal from EEG signals recorded using low resolution Emotiv device," in *Proc. IEEE Int. Conf. Syst., Man, Cybern.*, 2015, pp. 1445–1451.
- [6] R. Cooper, J. W. Osselton, and J. C. Shaw, *EEG Technology*, Oxford, U.K: Butterworth-Heinemann, 2014.
- [7] W. Philips, "Adaptive noise removal from biomedical signals using warped polynomials," *IEEE Trans. Biomed. Eng.*, vol. 43, no. 5, pp. 480–492, May 1996.
- [8] S. F. Abbasi, M. Awais, X. Zhao, and W. Chen, "Automatic denoising and artifact removal from neonatal EEG," in *Proc. IEEE 3rd Int. Conf. Biol. Inf. Biomed. Eng.*, 2019, pp. 1–5.
- [9] N. Barbara, T. A. Camilleri, and K. P. Camilleri, "A comparison of EOG baseline drift mitigation techniques," *Biomed. Signal Process. Control*, vol. 57, Mar. 2020, Art. no. 101738.
- [10] E. Prabhakararao and M. S. Manikandan, "On the use of variational mode decomposition for removal of baseline wander in ECG signals," in *Proc. IEEE 22nd Nat. Conf. Commun.*, 2016, pp. 1–6.
- [11] P. C. Lo and J.-S. Leu, "Adaptive baseline correction of meditation EEG," *Amer. J. Electroneurodiagnostic Technol.*, vol. 41, no. 2, pp. 142–155, 2001.
- [12] P. M. Alday, "How much baseline correction do we need in ERP research? Extended GLM model can replace baseline correction while lifting its limits," 2017, [arXiv:1707.08152](https://arxiv.org/abs/1707.08152).
- [13] L.-G. Zhou, H.-J. Li, and G.-S. Hu, "Real-time base-line drift correction and P-wave detection of ECG signal," in *Proc. IEEE Annu. Int. Eng. Med. Biol. Soc.*, 1989, pp. 49–50.
- [14] E. Tkacz, "A microcomputer based heart-rate variability analysis system," in *Proc. IEE Colloq. Technol. Progress Cardiol.*, 1990, pp. 9/1–9/7.
- [15] M. L. Riccio and J. C. Belina, "A versatile design method of fast, linear-phase FIR filtering systems for electrocardiogram acquisition and analysis systems," in *Proc. IEEE Comput. Cardiol.*, 1992, pp. 147–150.
- [16] N. V. Thakor and Y.-S. Zhu, "Applications of adaptive filtering to ECG analysis: Noise cancellation and arrhythmia detection," *IEEE Trans. Biomed. Eng.*, vol. 38, no. 8, pp. 785–794, Aug. 1991.
- [17] P. Strobach, K. A. Fuchs, and W. Harer, "Event-synchronous cancellation of the heart interference in biomedical signals," *IEEE Trans. Biomed. Eng.*, vol. 41, no. 4, pp. 343–350, Apr. 1994.
- [18] S. Agrawal and A. Gupta, "Fractal and EMD based removal of baseline wander and powerline interference from ECG signals," *Comput. Biol. Med.*, vol. 43, no. 11, pp. 1889–1899, 2013.
- [19] P. Gupta, K. K. Sharma, and S. D. Joshi, "Baseline wander removal of electrocardiogram signals using multivariate empirical mode decomposition," *Healthc. Technol. Lett.*, vol. 2, no. 6, pp. 164–166, 2015.
- [20] S. Lahmiri, "Comparative study of ECG signal denoising by wavelet thresholding in empirical and variational mode decomposition domains," *Healthc. Technol. Lett.*, vol. 1, no. 3, pp. 104–109, 2014.
- [21] N. Pan, V. Mang, M. P. Un, and P. S. Hang, "Accurate removal of baseline wander in ECG using empirical mode decomposition," in *Proc. IEEE Int. Conf. Funct. Biomed. Imag.*, 2007, pp. 177–180.
- [22] M. Shahbakhthi, H. Bagheri, B. Shekarchi, S. Mohammadi, and M. Naji, "A new strategy for ECG baseline wander elimination using empirical mode decomposition," *Fluctuation Noise Lett.*, vol. 15, no. 2, 2016, Art. no. 1650017.
- [23] R. D. Gavas, S. R. Tripathy, D. Chatterjee, and A. Sinha, "Cognitive load and metacognitive confidence extraction from pupillary response," *Cogn. Syst. Res.*, vol. 53, pp. 325–334, Dec. 2018.
- [24] K. Dragomiretskiy and D. Zosso, "Variational mode decomposition," *IEEE Trans. Signal Process.*, vol. 62, no. 3, pp. 531–544, Feb. 2013.
- [25] N. Yeung, R. Bogacz, C. Holroyd, S. Nieuwenhuis, and J. Cohen, "Simulated EEG data generator." 2019. [Online]. Available: <https://data.mrc.ox.ac.uk/data-set/simulated-eeg-data-generator>
- [26] M. S. Treder, A. Bahramisharif, N. M. Schmidt, M. A. J. Van Gerven, and B. Blankertz, "Brain-computer interfacing using modulations of alpha activity induced by covert shifts of attention," *J. Neuroeng. Rehabil.*, vol. 8, no. 1, pp. 1–10, 2011.
- [27] X. Ning, I. W. Selesnick, and L. Duva, "Chromatogram baseline estimation and denoising using sparsity (BEADS)," *Chemometr. Intell. Lab. Syst.*, vol. 139, pp. 156–167, Dec. 2014.
- [28] R. Gavas, D. Jaiswal, D. Chatterjee, V. Viraraghavan, and R. K. Ramakrishnan, "Multivariate variational mode decomposition based approach for blink removal from EEG signal," in *Proc. IEEE Int. Conf. Pervasive Comput. Commun. Workshops (PerCom Workshops)*, 2020, pp. 1–6.

**SHIREEN FATHIMA** was born in Raichur, India. She received the bachelor's degree in electronics and communication engineering from the SLN College of Engineering, Raichur, in 2012, and the master's degree in electronics from the HKBK College of Engineering, Bengaluru, India, with First Rank Gold Medal at the university level of Visvesvaraya Technological University in 2014.

She is a Research Scholar with the Faculty of Electrical and Electronics Engineering Sciences, Visvesvaraya Technological University, Belagavi, India. She has seven years of teaching experience and is currently working as an Assistant Professor with the HKBK College of Engineering. She has published papers in several reputed journals and presented papers in many conferences. Her areas of interest include biomedical signal processing, image processing, embedded systems, and Internet of Things.

Ms. Fathima is a Life Member of the Indian Society for Technical Education.

**MAAZ AHMED** was born in Bengaluru, India. He received the master's degree (First Rank) in digital electronics and communication from M. S. Ramaiah Institute of Technology, Bengaluru, in 2010, and the Ph.D. degree in electrical and electronics sciences from Visvesvaraya Technological University, Mysuru, India, in 2018.

He has nine years of teaching and research experience and is currently working as an Associate Professor with the HKBK College of Engineering, Bengaluru. He has published many papers in several reputed journals and presented papers in many conferences. His areas of interest include signal processing, HPC, computer architecture, and image processing.

Dr. Ahmed is a member of the Indian Society for Technical Education and IETE.